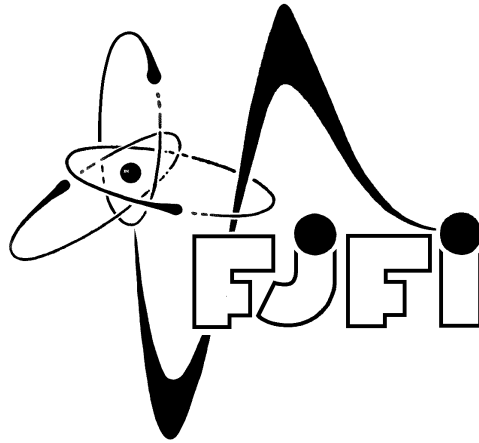


CZECH TECHNICAL UNIVERSITY IN PRAGUE  
Faculty of Nuclear Sciences and Physical Engineering



# Technical Design Report

Spark chamber

PPRA collaboration  
class of 2015/2016

# PPRA collaboration

*Project coordinator*

**Matouš Vozák**

*Spokesperson*

**Zbyněk Nguyen**

\*\*\*

*External construction*

**Hana Hruběšová**

**Miroslav Šaur**

*Internal construction*

**Jakub Kvapil**

**Ota Zaplatílek**

*Fill gas*

**Alena Harlenderová**

**Martin Kocmánek**

*Trigger and scintillators*

**Michal Kocan**

**Matouš Vozák**

*Theory and simulations*

**Filip Nechanský**

*Power supply*

**Jan Vaněk**

**Zbyněk Nguyen**

# Contents

<b>Introduction</b>	<b>1</b>
<b>1 Construction</b>	<b>2</b>
1.1 External construction . . . . .	2
1.2 Internal construction . . . . .	3
1.2.1 Gas inlet and outlet . . . . .	3
<b>2 Fill gas</b>	<b>5</b>
2.1 Gas injection . . . . .	5
2.2 Gas proportional can . . . . .	5
2.2.1 Experimental setup . . . . .	5
2.2.2 Testing . . . . .	7
<b>3 Trigger</b>	<b>9</b>
3.1 Detection and signal conversion . . . . .	9
3.2 Signal amplification . . . . .	10
3.2.1 Preamplification . . . . .	11
3.2.2 Low voltage amplification . . . . .	11
3.2.3 High voltage amplification . . . . .	11
3.3 Transformer . . . . .	14
3.4 Spark gap . . . . .	15
3.5 Power supply . . . . .	15
3.5.1 HV supply . . . . .	15
3.5.2 Clearing voltage . . . . .	16
<b>4 Summary</b>	<b>17</b>
<b>Bibliography</b>	<b>18</b>

# Introduction

There is a vast amount of high-energy particles flying towards Earth, coming from outer space. As these particles interact with our atmosphere, they produce the so-called secondary cosmic rays. Among the decay products, pions  $\pi^\pm$  and kaons  $K^\pm$  can be found, which subsequently decay mostly into muons  $\mu^\pm$  – via reactions  $\pi^- \rightarrow \mu^- + \bar{\nu}_\mu$ ,  $\pi^+ \rightarrow \mu^+ + \nu_\mu$ ,  $K^- \rightarrow \mu^- + \bar{\nu}_\mu$  and  $K^+ \rightarrow \mu^+ + \nu_\mu$ .

Muons are of particular interest in this project. Firstly, due to having large mass, they penetrate matter easily and lose lesser amount of energy through bremsstrahlung. Secondly, the muon flux at the surface of the Earth is particularly high, with a value of  $70 \text{ m}^{-2} \text{ s}^{-1} \text{ sr}^{-1}$  [2]. Therefore, they are easily detectable in lower altitudes. The spark chamber detector was chosen as a plausible way of detecting these muons and visualising their path.

This document contains the technical aspects of the spark chamber project. The concept was introduced in [1]. However, some changes had to be made in contrast with the first ideas due to optimization of apparatus and technical difficulties. Namely, the gas has been changed from He to Ar, dimension of bottom box has been extended from  $50 \times 50 \text{ cm}^2$  to  $70 \times 50 \text{ cm}^2$ , the inner plates are made from copper PCB and they are attached not only by one rod but also with plastic dilator. The transformer with desired parameters had to be made from scratch. Instead of beagle-bone black, own circuits were built and used. The low and high voltage protection in power supply had to be done by capacitors and resistors. Although all the materials have been assembled, the spark chamber has not been completed and tested.

The text is structured as follows. In the first chapter, external and internal construction is characterized. The second chapter is focused on the gas used as the chamber fill, including the description of a preliminary detector to test the gas performance. The third chapter is dedicated to trigger circuit description, including the power supply.

# Chapter 1

## Construction

### 1.1 External construction

The idea was to design a spark chamber in a representative way with a condition that sparks could be clearly visible by a naked eye (Fig. 1.1). The overall size of the structure is approximately  $40 \times 60 \times 60 \text{ cm}^3$  ( $\mathbf{h} \times \mathbf{w} \times \mathbf{l}$ ). Experiment consists of a box with active volume in which measurements take a place, pedestal where important parts of apparatus are stored and a wooden desk for stability and easier transport.

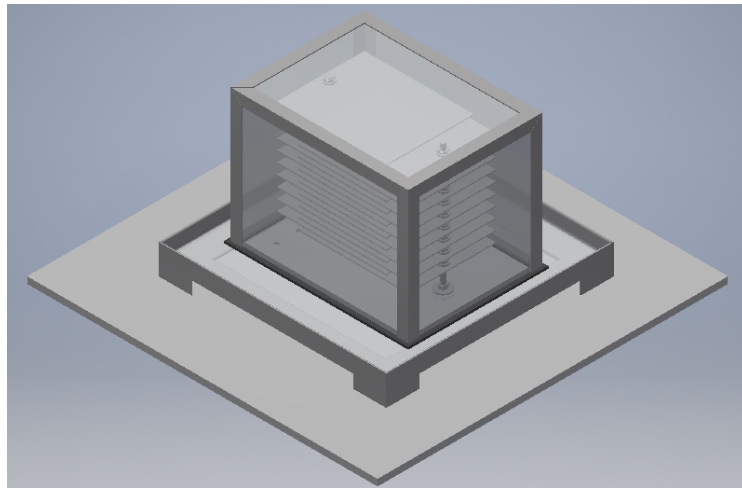


Fig. 1.1: Render of the spark chamber, isometric view. [6]

The box is made out of polymethyl methacrylate (PMMA also known as plexiglass) due to its transparency, low weight, and an easy access. Dimensions of the box are  $25 \times 30 \times 40 \text{ cm}^3$  ( $\mathbf{h} \times \mathbf{w} \times \mathbf{l}$ ) with a removed base. Walls of the box were connected together using glue Acrifix 190 for its good isolation property, easy manipulation and relatively cheap prize. Two holes were drilled in the walls of the box for gas inlet and outlet. The box is standing on the PMMA pedestal with dimensions of  $50 \times 70 \times 7 \text{ cm}^3$ . The seal between the box and the pedestal is realized via U-Profil with rubber insulation screwed to the pedestal Fig. 1.3. Several holes were made in the top wall of the pedestal for the junction with the box, power rods and wiring. However, the rest of the walls of the pedestal have not been cut yet thus not glued together as well.

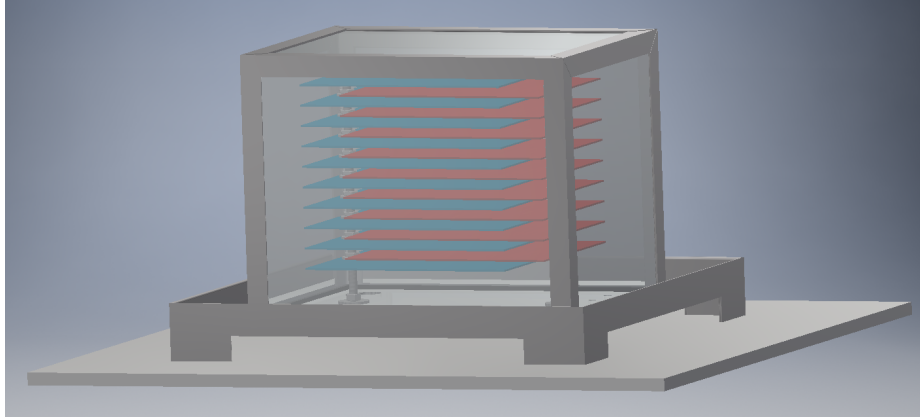


Fig. 1.2: Render of the spark chamber with inner electrodes highlighted. Colours represent electrodes of same polarity. [6]

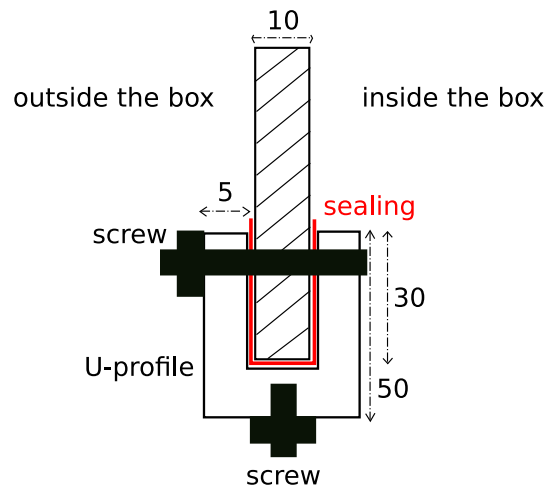


Fig. 1.3: Junction between the box and pedestal. All the values in the figure are in millimeters, using the U-profile.

## 1.2 Internal construction

There are 20 cuprexit plates in two rows (for two polarities) by 10 inserted in the PMMA box, so as to create an electric field to provide the necessary energy for sparks to occur (Fig. 1.2). Cuprexit plates have dimensions  $300 \times 200 \times 1.5 \text{ mm}^3$  and are made of durable polymer with  $35 \mu\text{m}$  copper layer deposited on the both sides of plates. There are two M10 steel rods for each row to which plates are fixed by steel washers and nuts. The placement of the rods in the plates is shifted from the detection area of  $200 \times 200 \text{ mm}^2$  Fig. 1.4. There are two  $40 \times 10 \times 10 \text{ mm}^3$  blocks made of PMMA between each plates in the corner on the opposite side of the plate than a rod for better stability of the system. The blocks are glued to the plates using a superglue. A PVC isolating tape with dielectric strength of 1000 V and an ordinary insulating tape were used to cover the edges of cuprexit plates to prevent electric discharge near the edges of plates and walls of the box.

### 1.2.1 Gas inlet and outlet

The working gas is brought from the source bottle to the PMMA box by polyurethane tube through  $1/4''$  brass ball valve, standard manometer with lower outlet and threaded



# Chapter 2

## Fill gas

The performance of the spark chamber is highly affected by the gas composition in the chamber. The voltage between the electrodes should not exceed the breakdown voltage of the gas. Therefore, knowledge of the characteristics of the selected gas is required in order to avoid detecting fake events. Behaviour of gasses, in particular their breakdown voltage, which might be used in the spark chamber were studied in the conceptual design report in [1, Chap. 2]. Helium and argon were considered as the fill gases because of their low breakdown voltage 4.7 kV/cm [3] and 5.6 kV/cm [3] respectively, and also because of their relatively low prize (hence the ease of access). Eventually, argon was chosen over helium as a chamber fill because of the lower probability of leakage. The average energy required to create an electron-ion pair in argon is about 26 eV [4], that is a sufficient value for creation a large amount of electron-ion pair from a passing muon.

### 2.1 Gas injection

The aim is to have as much concentration of argon as possible because of the different breakdown voltages of other gasses which may cause early quenching of sparks. It is not possible to obtain a high quality vacuum as the spark chamber is not designed to withstand low pressures. In order to reduce the concentration of other gasses, argon is slowly pushed to the chamber through a gas inlet. Meanwhile, gas is also being drained on the other side of the chamber for a certain period of time, using a vacuum pump. The time interval needed to obtain a sufficient concentration is roughly estimated in the next chapter. The gas pressure in the chamber will be slightly higher than atmospheric pressure to prevent outside gasses from entering the apparatus.

### 2.2 Gas proportional can

In order to study properties of argon experimentally, another simple gas detector made of can was built before the completion of the spark chamber. The main motivation for the gas proportional can was to build a properly working device at a minimal cost to test mainly dependence of discharge rate on the voltage and source of radiation. A good option for a cheap conducting cathode tube is a conventional aluminium beverage can. The wall thickness is thin enough for low energetic  $\gamma$ ,  $X$ -rays and of course muons. The detector was designed and built with inspiration from [5], [4].

#### 2.2.1 Experimental setup

The main component is the aluminium beverage can of length  $l_c = 133.5$  mm, outer diameter  $d_{outer} = 53$  mm and wall thickness  $h = 0.25$  mm, leading to the inside volume of approximately  $V = 330$  ml. Both end caps were removed, edges were rubbed off and the

inside was thoroughly cleaned. Two square-shape covers made of PMMA were used as new end caps, with side length  $a = 80$  mm and thickness  $h_{ec} = 5.9$  mm.

A small plastic cylinder (length  $l_c = 12$  mm and diameter  $d_c = 6$ ) with a centre hole was glued to each end cap as an attachment for the anode wire of length  $l_w \approx 150$  mm, diameter  $d_w = 0.15$  mm. This wire was obtained by taking a single strand from a conventional steel cable and checked for possible surface irregularities.

To secure this construction, four threaded metal rods (length  $l_{tr} = 156$  mm, diameter  $d_{tr} = 3.8$  mm) and 16 nuts were used. At every seam, adhesive super glue was applied to ensure airtightness. The wire is soldered to the high voltage cable, low voltage cable is soldered at the surface of the can, after removing the colour coating. Gas supply with two valves and pressure gauge (0 – 1.6 bar) was connected to the end caps using gas tubing (inner diameter  $d_{inner} = 2$  mm). The filling gas (Ar) was kindly provided by Department of Nuclear Chemistry, FNSPE CTU.

The experimental setup of gas proportional can is depicted in Fig. 2.1 and Fig. 2.2.

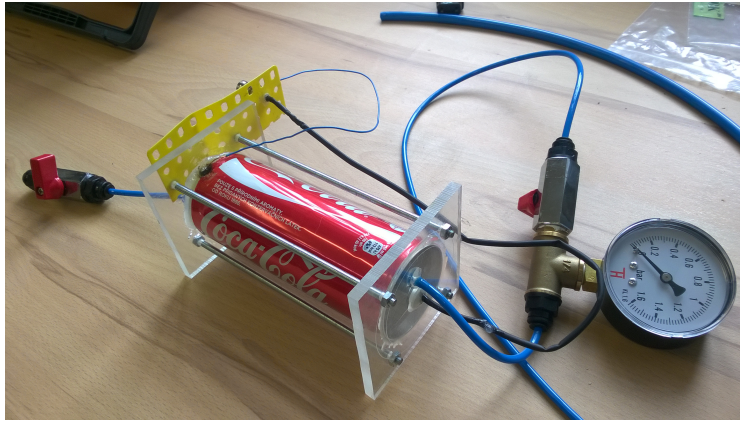


Fig. 2.1: Experimental setup of gas proportional can.



Fig. 2.2: Gas proportional can, end cap detail.

### 2.2.2 Testing

High voltage supply, detector, oscilloscope, resistors and capacitor were connected together as shown in the Fig. 2.3 and 2.4. The operating voltage was calculated from

$$U(r) = E(r) \ln(b/a) \cdot r, \quad (2.1)$$

where  $U$  is voltage,  $b$  radius of can,  $a$  radius of the wire and  $E(r)$  is electric intensity. For radius  $r = a + 1$  mm, the voltage was calculated to be 531 V, under requirement that intensity is at least  $10^6 \text{ Vm}^{-1}$ .

The can was filled to the pressure of 2 bar and the gas filling 1 minutes. A simple extrapolation (presuming the speed of the filling) of this leads to a very rough estimate of the filling of the spark chamber – approximately 1.5 hours in the ideal case per filling cycle.

Visible signal from the can was measured with different applied voltage as can be seen in Fig 2.5 and 2.6. As expected, the pulse rises with rising of applied voltage. However, when strong  $\beta^-$  source, namely  $^{99}\text{Tc}$  was put close to the can, no significant additional activity was observed. This might be caused by high intensity of photo-effect electrons, since transparent sides of the can were not properly shielded. Therefore, further investigation is required to understand the behavior of the can and to measure the properties of argon. The pulses exhibit proportional behavior.

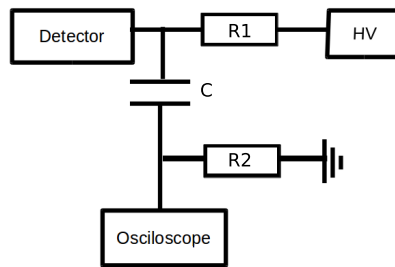


Fig. 2.3: Block scheme of the gas proportional can circuit.  $R1 = 6 \text{ M}\Omega$ ,  $R2 \sim 10 \text{ }\Omega$  (measured resistance of the grounding wire),  $C = 2200 \text{ pF}$ .

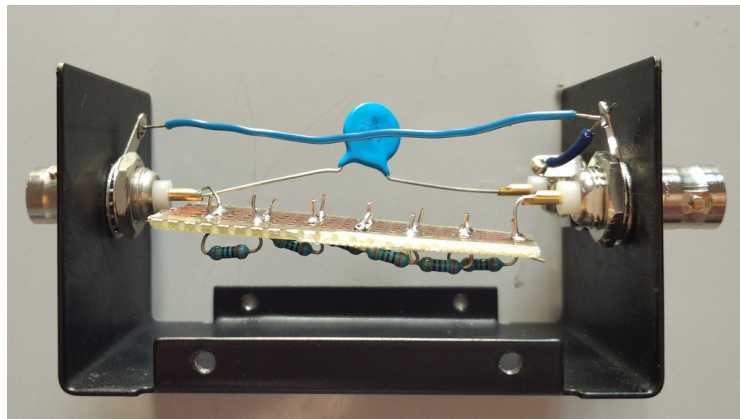


Fig. 2.4: Photo of the gas proportional can circuit (see Fig. 2.3). The blue round part is the capacitor, resistors are connected in series using the circuit board ( $6 \times 1 \text{ M}\Omega$ ), upside down on the photo

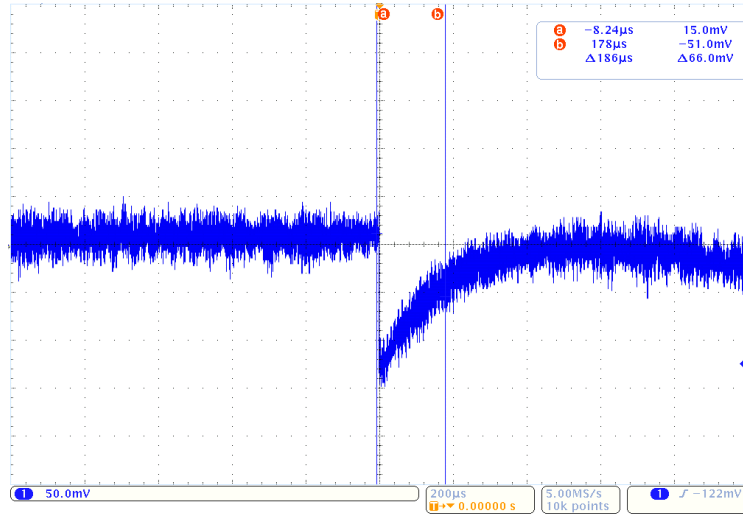


Fig. 2.5: Signal from the can when 500 V was applied. The amplitude is roughly 150 mV.

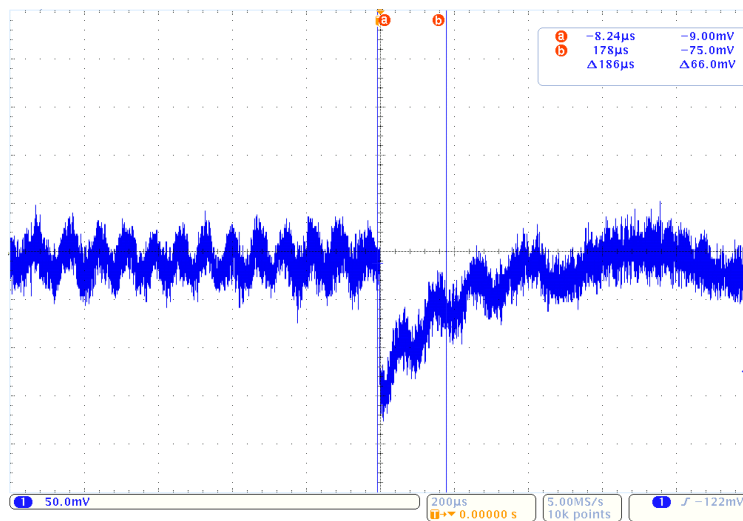


Fig. 2.6: Signal from the can when 1400 V was applied. The amplitude is roughly 175 mV.

# Chapter 3

## Trigger

The events of interest are those with muon passing through all the layers of detector. In order to be capable of determining and measuring such events, the trigger system was designed. Simplified functionality of the trigger system is depicted in Fig. 3.1. Main functions of the trigger are the following: to select the events of interest and modify the received signal to make a suitable conditions for the detection. At first, particle is detected in a scintillator, which gives a light signal. This signal is then converted into electric signal in a photomultiplier. The next stage is an amplification of the signal which can be divided into three parts – preamplification, low voltage amplification and high voltage amplification (Fig. 3.3).

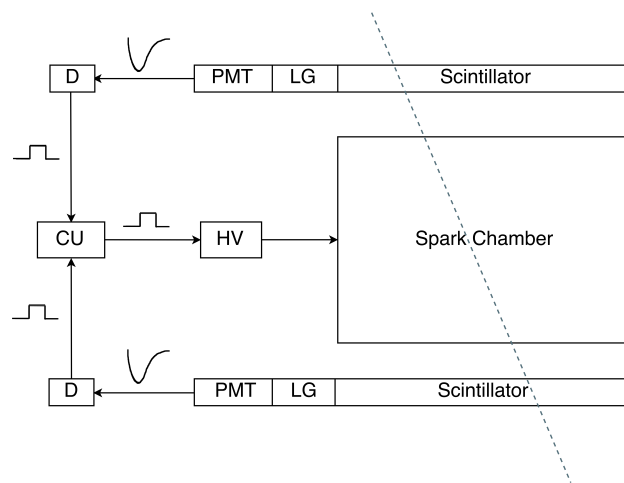


Fig. 3.1: Trigger circuit. LG = Lightguide, PMT = Photomultiplier tube, D = Discriminator, CU = Coincidence unit, HV = High voltage supply. Dashed line represents the muon trajectory.

### 3.1 Detection and signal conversion

The first part of the trigger system is a scintillator. As particles propagate through scintillator they deposit energy which is emitted in a form of photons. Both scintillators in use are made by Nuvia [7] and their characteristics can be found in Tab. 3.1. They were saw cut to the required active area of the electrode plates  $20 \times 20 \text{ cm}^2$ . To determine the width of the scintillator, simulations were carried out to investigate the amount of energy

deposited by muons (1-200 GeV) in the scintillator [1, Sect. 4.1]. It was found out that the particles leave around 4 MeV in 2 cm wide scintillator, which is a sufficient value.

Density	1.03 g/cm <sup>3</sup>
Index of refraction	1.57
Softening point	70-75°
Luminous flux (power)	65° (in comp. with anthracen)
Afterglow duration	2.5 ns
Maximal wavelength	420-440 nm

Tab. 3.1: Characteristics of the scintillator. [8]

Photons from scintillator are collected at a photomultiplier (PMT) where the light is converted to electric signal. Typical shape of PMT output in case of event detection can be found in Fig. 3.2. The rest of its characteristics are in [9]. Plastic lightguide was used to connect scintillator with PMT in order to raise the detection efficiency since the PMT diameter is 5 cm. Simulations of the scintillator efficiency can be found in [1, Sect. 4.1] as well.



Fig. 3.2: Measured pulse from the photomultiplier.

## 3.2 Signal amplification

In order to bring a sufficient voltage (in order of kV, given by the properties of gas (see Chapter 2) to the electrodes, the HV supply is used, and it is driven by the PMT signal (in order of mV). Signal has to be shorter in less than  $\sim 1 \mu\text{s}$  with fast rise time  $\sim 0.1 \mu\text{s}$  [13], [14], otherwise the electron-ion pairs created by the passing muon recombine and the signal will be lost. Also, HV rise should be very sharp – its duration should be in the order of nanoseconds. This is why the spark gap is used. In other words, there will be no spark discharge. The signal is enhanced by various components and methods described in the subsections below.

### 3.2.1 Preamplification

The described circuit is in Fig. 3.3. At first, the signal from photomultiplier is brought to an inverting operational amplifier LM318. The amount of signal enhancement is regulated using the resistors R1, R2 and potentiometer POT1 (R7, R8 and POT3 in the second branch). R3 and R4 (R9 and R10) divide the voltage at the positive input of the amplifier. The signal, being amplified approximately 10 times, goes to a comparator which selects the "good" events with the amount of the signal above setup threshold  $\sim 6.5$  V. R5, R6 and POT2 (R11, R12, POT4) serve as a voltage divider for the reference voltage of the comparator. When the signal exceeds the threshold, comparator sends rectangular shape pulse to a coincidence unit, described later on, which sends the signal only if it received overlapping signals from both scintillators.

### 3.2.2 Low voltage amplification

The inspiration for the following circuit was taken from [?]. The signal in a low voltage part of the circuit is amplified from 5 V up to inverted 300 V. The circuit consists of 3 steps: first coincidence between both scintillators is done with AND integrated circuit (labeled Y1), second amplification from 5 V to 12 V is done by PNP bipolar transistor and finally IGBT transistor amplify the signal up to inverted 300 V.

The coincidence unit provided by AND integrated circuit takes 2 rectangular 5 V pulses and sends 20 ns delayed 5 V rectangular pulse. The R13 resistor acts as a high current protection and T1 NPN bipolar transistor acts as a galvanic divider to protect both parts. PNP bipolar transistor is an amplifier from 5 to 12 V triggered by 5 V on the gate. The 5 V is given by voltage divider constructed by resistors R14 and R15 since common 12 V power supply is used. Resistors R16, R17 and R18 acts as a voltage and a current protection. Photo of the circuit can be seen in Fig. 3.5.

Insulated-gate bipolar transistor (IGBT) T3 is used as an amplifier from 12 V to inverted 300 V. The 300 V are taken from the 240 V grid, rectified by full wave single phase rectifier, supported by resistor to protect a fuse from turn-on current spike. This spike occurs due to the charging of C6. Capacitors C5 and C6 are used to ensure stable voltage in circuit and cover transistors voltage drops. The resistor R19 is a current protection and diodes D1 and D2 provides required pulse polarity. In order to filter the DC offset from a pulse a coupling, capacitor C7 is used. Photo of the circuit can be seen in Fig. 3.5. The resulting  $-300$  V pulse is the input for a part of the circuit with an amplification to a high voltage.

### 3.2.3 High voltage amplification

As mentioned before, it is necessary to provide a relatively high voltage in a very short time. Up to now the signal has  $-300$  V which is still not enough. Therefore, it is sent to a HV circuit (Fig. 3.7) which contains a transformer and a spark gap.

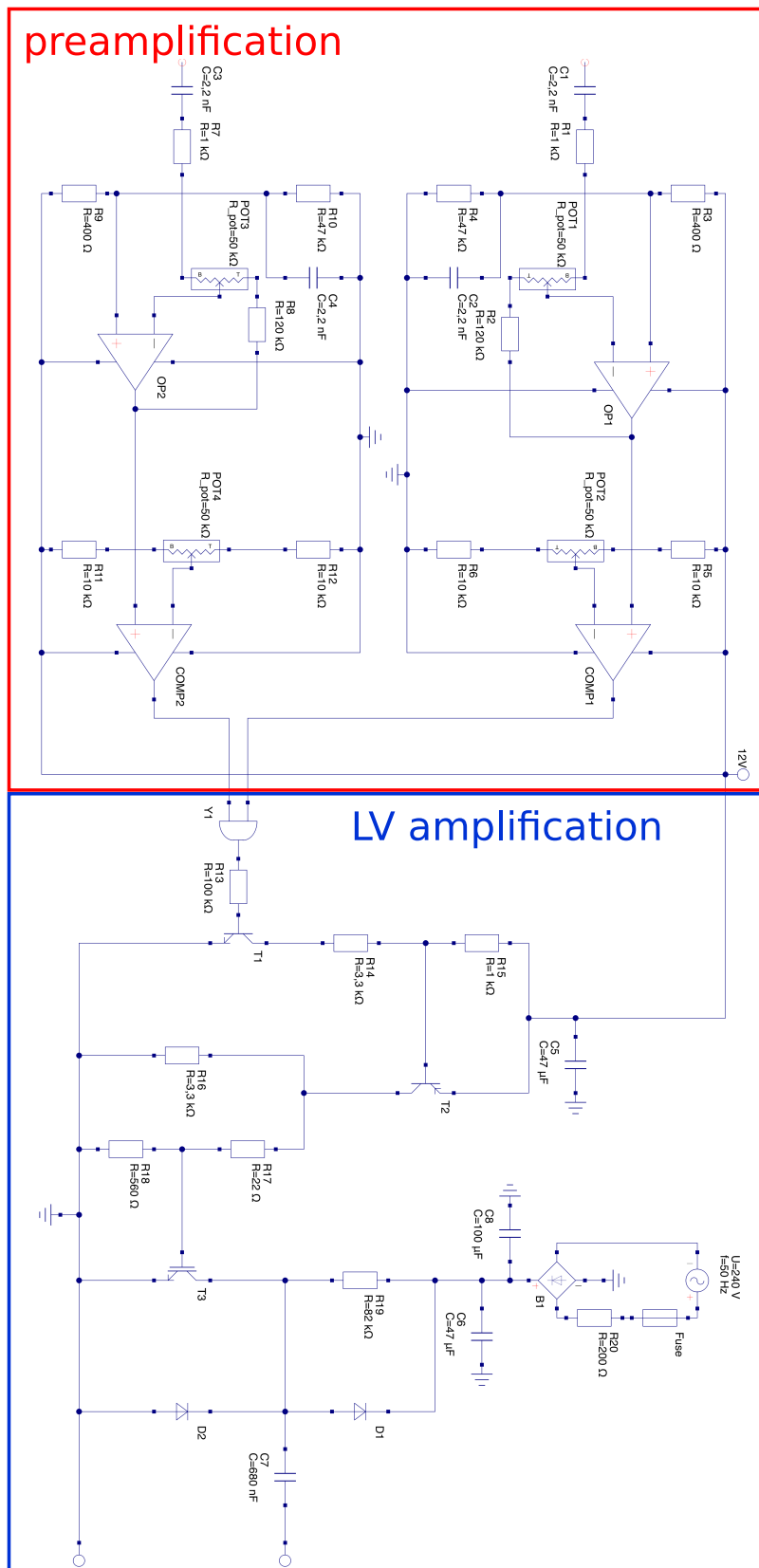


Fig. 3.3: Circuit for amplification of the photomultiplier signal from mV up to 5 V in preamplifier region and from 5 V to  $-300$  V.



Fig. 3.4: Blue: signal before the IGBT. Cyan: signal before the coincidence unit.

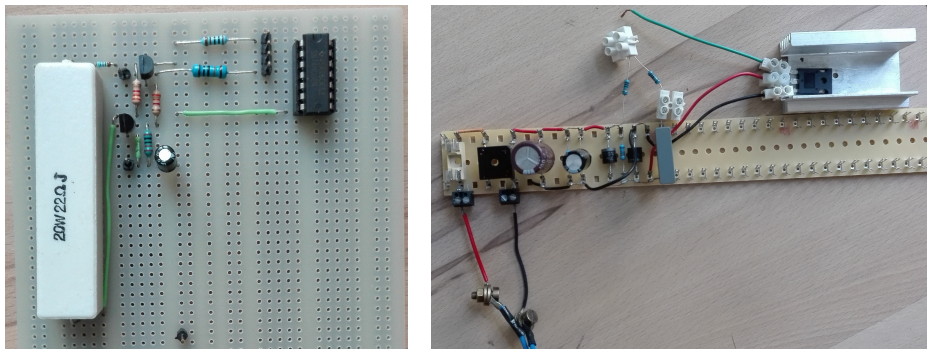


Fig. 3.5: Left: Photo of the 5 V to 12 V amplifier. Right: Photo of the 12 to -300 amplifier. IGBT transistor is mounted on an aluminum cooler.

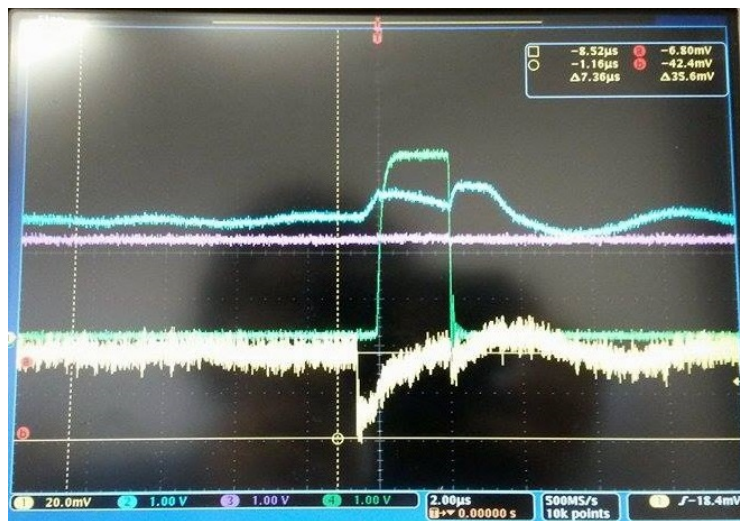


Fig. 3.6: Signal from the amplification circuit. Yellow represents the pulse from the photo-multiplier, blue is the photomultiplier output, green is the comparator output and violet is the reference value of the oscilloscope.

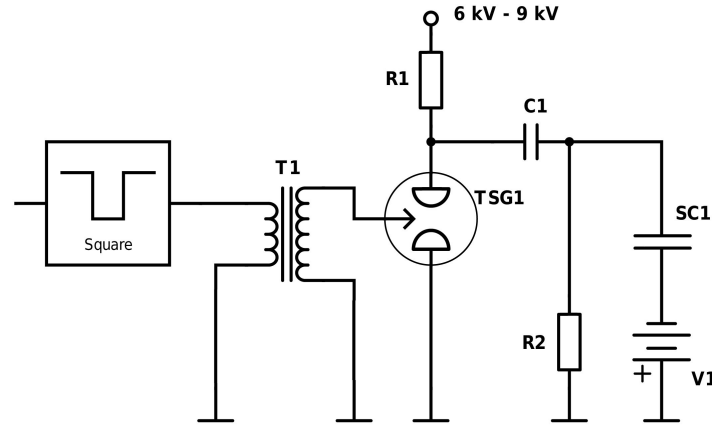


Fig. 3.7: Simplified scheme of the HV supply for the spark chamber. Square refers to the 300 V pulse from the LV amplification part of the circuit; T1 is the transformer; TSG1 is triggered spark gap; R1 = 11.2 M $\Omega$  and R2 = 10 k $\Omega$  are resistors; C1 = 3.33 nF is a capacitor; V1 is the LV source and SC1 represents the spark chamber.

### 3.3 Transformer

At first the  $-300$  V signal is stepped-up by the transformer (T1 in Fig. 3.7). It consists of two solenoids connected to the same ferrite core. The characteristics of the ferrite material can be found in Tab. 3.2. The primary coil has  $N_p = 8$  turns and it is made of enamelled copper wire with 0.8 mm diameter, the secondary coil has  $N_s = 80$  turns and it is made of enamelled copper wire with 0.2 mm diameter. The coils are wound directly at the ferrite core coated with PVC insulating tape. The whole transformer is then covered using the same tape as shown in Fig. 3.8. Using the winding ratio equation as an approximation,

$$\frac{V_p}{V_s} \approx \frac{N_p}{N_s}, \quad (3.1)$$

where  $V_p$  and  $V_s$  are voltages at the primary and secondary winding, respectively, the voltage should be increased approximately 10 times. Another important parameter of the transformer is the time delay between input and output signal. This delay was found to be negligible, therefore not causing any significant delay in the signal propagation.

Initial permeability	125
Maximum permeability	450
Max flux density at 800 A/m	0.235 T
Volume resistivity	$10^8 \Omega\text{cm}$
Loss factor at 2.5 MHz	$32 \cdot 10^6$
Coercive force	130 A/m
Curie temperature	350 $^\circ\text{C}$

Tab. 3.2: Selected characteristics of ferrite core [10].

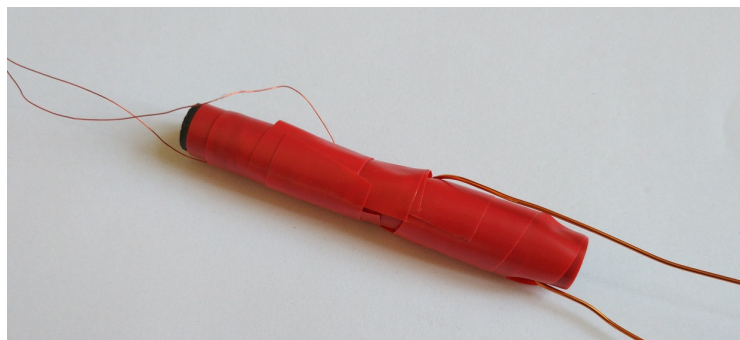


Fig. 3.8: Photo of the transformer.

### 3.4 Spark gap

In order to deliver the HV from the HV supply into the chamber, a simple spark gap is employed (TSG1 in Fig. 3.7). The purpose of the spark gap is to enable quick triggering of external HV source. According to [15] the delay caused by the spark gap should be around  $\approx 20$  ns. Main drawback is that the difference between the input and output voltage cannot be that large.

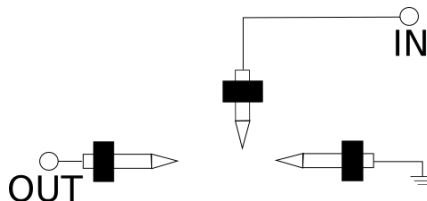


Fig. 3.9: Configuration of nodes of the spark gap trigger (detail from Fig. 3.7). IN is the transformer output, OUT is connected to the HV supply. Distances between the tips are set in a way that between IN and GND, the spark discharges spontaneously and between OUT and GND not. However, if the spark between IN and GND occurs, it will trigger a spark between OUT and GND as well.

The spark gap consists of three nodes arranged as in Fig. 3.9, where the distance between the nodes is based on the input and output voltage. Originally the spark gap was to be mounted on a wood base, however when the concept was tested, it was found that the voltage discharged through the wood base instead of air. Therefore, a PMMA base was chosen as a substitute.

The breach of the gaps was tested using Wimshurst machine [11] and Van de Graaff generator [12], where the former functions as a trigger and the latter as an voltage output. The spark gap functioned as expected for this setup, although it was not yet tested with the LV input.

## 3.5 Power supply

### 3.5.1 HV supply

Technix SR120KV-300W power supply [16] with maximum voltage of 120 kV is used as a HV source. Voltage up to 9 kV is delivered to the spark gap. The highest voltage is limited by capacitor C1 in Fig. 3.7, which is able to sustain maximum voltage of 9 kV (C1 consists of 3 ceramic capacitors with maximum voltage of 3 kV [17]).

### 3.5.2 Clearing voltage

Clearing voltage is a low voltage applied permanently to the plates of the spark chamber, collecting remaining ions after the spark discharge is quenched. It prevents unwanted recombination of ions before the signal from trigger arrives.

For 1 detection per second, the sufficient voltage should be in order of tens of volts [13], having considered the velocity of charge carriers in metal. The voltage is delivered by four standard 9 V batteries connected in series at one set of plates (V1 in Fig. 3.7), the high voltage pulse is applied at the remaining set of plates. The advantages are simplicity of the LV supply and the galvanic independence between the LV and HV supplies. Moreover, the low voltage can be easily increased by using more batteries in case that the clearing voltage efficiency decreases during the spark chamber lifetime.

# Chapter 4

## Summary

The main body of the detection chamber has been put together except the lid which has not been glued yet to the rest of the body. However, all the holes for the gas inlet and outlet and for the U-profiles are already prepared. From the pedestal, only the top wall with the holes for the wiring, steel rods and profiles are prepared. Other four walls of the pedestal need to be cut to desired dimensions and glued together. Considering the inner structure of the chamber, all the electrode plates have been covered by insulating tapes and holes for the steel rods have been drilled. The PMMA blocks for the stability of the apparatus are prepared as well.

The gas proportional can was constructed and already used for measurement of argon properties. A visible signal with a proportional character was measured when high voltage was applied. Nevertheless, further measurements are required in order to study the behavior of the can as a proportional chamber.

All the components of the trigger circuit have been assembled and put to tests individually. Unfortunately, the preamplifier section needs further investigation of the signal amplification due to technical difficulties. However, the LV part is complete and prepared for tests with signal from preamplifier. Regarding the HV amplification, coil has been winded up and it should give a signal amplified approximately 10 times. Measurement of the real amplification is yet to be done. Spark gap as a final part of the trigger was constructed and tested using a lab equipment. Unfortunately the signal propagation through the whole trigger has not been tested, mainly due to the mentioned difficulties with preamplifier.

As for now, major steps towards the construction of the spark chamber have been made. All the parts have been assembled and some of the parts are already in the final state. What is left is to finish the construction, test the output of some constructed parts to determine whether they agree with the theoretical assumptions and finally, the measurement with the whole apparatus itself.

The spark chamber team would like to take this opportunity and thank all who contributed to the project with valuable ideas. Namely the supervisors Ing. Jaroslav Adam, Ph.D. and Ing. Jan Čepila, Ph.D.

# Bibliography

- [1] COLLECTIVE OF AUTHORS, *Conceptual design report, Spark Chamber*, (2016), [accessed 9/2016], [http://physics.fjfi.cvut.cz/files/predmety/02PPRA/Docs/cdr\\_2015-16.pdf](http://physics.fjfi.cvut.cz/files/predmety/02PPRA/Docs/cdr_2015-16.pdf)
- [2] K.A. OLIVE ET AL., *Review of Particle Physics – Cosmic Rays*, Chin. Phys. C, **38**, 090001, (2014) and 2015 update, [accessed 1/2016] <http://pdg.lbl.gov/2015/reviews/rpp2014-rev-cosmic-rays.pdf>
- [3] A.K.,VIJH, *Communication on the Relative Electric Strengths and the Molecular Weights of Gases, Electrical Insulation*, IEEE Transactions on, Volume EI-12, Issue 4, pp 313-315, (1977), DOI: 10.1109/TEI.1977.297984
- [4] A. WINKLER, A. KARADZHINOVA, T. HILDÉN, F. GARCIA, G. FEDI, F. DEVOTO AND E. J. BRÜCKEN, *A gaseous proportional counter built from a conventional aluminium beverage can*, Am. J. Phys. **83** (2015) 733, [arXiv:1509.02379 [physics.ed-ph]].
- [5] JUSKA, KATARINA, LA' IS, MORTEN, *Proportional Counter*, (2016)
- [6] *Render of the spark chamber*, courtesy of Stanislav Škoda
- [7] NUVIA, *Official website*, [accessed 1/2016], <http://www.nuvia.cz/en>
- [8] NUVIA, *Plastic scintillators*, [accessed 1/2016], <http://146-2-13-46.tmcz.cz/index.php/en/sluzainze-en/scintilaci-materialy-en/plast-scintilator>
- [9] ET ENTERPRISES, *9266B Photomultiplier specifications*, (2010), [accessed 13.1.2016], <https://my.et-enterprises.com/pdf/9266B.pdf>
- [10] AMIDON CORP., *Magnetic properties of ferrite materials*, (2003), [accessed 20.9.2016], [http://www.amidoncorp.com/product\\_images/specifications/2-03.pdf](http://www.amidoncorp.com/product_images/specifications/2-03.pdf)
- [11] WIKIPEDIA, *Wimshurst machine*, [accessed 25.9.2016], [https://en.wikipedia.org/wiki/Wimshurst\\_machine](https://en.wikipedia.org/wiki/Wimshurst_machine)
- [12] WIKIPEDIA, *Van de Graaff generator*, [accessed 25.9.2016], [https://en.wikipedia.org/wiki/Van\\_de\\_Graaff\\_generator](https://en.wikipedia.org/wiki/Van_de_Graaff_generator)
- [13] J. COLLINS, *Construction of a Prototype Spark Chamber* Press, New York, (1967). arXiv:1010.4010
- [14] J. W. CRONIN, *Bubble and Spark Chambers*, Academic Press, New York, (1967).
- [15] COLLECTIVE OF AUTHORS, *Construction and Evaluation of a Fast Switching Trigger Circuit for a Cosmic Ray Detection Spark Chamber*, (2009), [accessed 22.1.2016], <http://www.hep.phy.cam.ac.uk/~lester/dtm662/forDavid/HastilyPutTogether.pdf>

- [16] TECHNIX HIGH VOLTAGE COMPANY, *DC High Voltage Generators, 300 W to 3 kW SR Series, From 300 V to 200 kV output voltage*, (2015), [visited 14.10.2015], [http://www.technix-hv.com/technix/sites/default/files/downloads/DATASHEET\\_SR-300-3000-W-SERIES\\_ENG.pdf](http://www.technix-hv.com/technix/sites/default/files/downloads/DATASHEET_SR-300-3000-W-SERIES_ENG.pdf)
- [17] SR PASSIVES, *Ceramic disc capacitor 3kV datasheet*, (2016), [visited 25.9.2016], [http://www.ges.cz/sheets/c/cck3k\\_xx.pdf](http://www.ges.cz/sheets/c/cck3k_xx.pdf)